



**Quantum impurities
from mobile Josephson junctions to depletions**

Schechter, Michael; Gangardt, Dimitri M.; Kamenev, Alex

Published in:
New Journal of Physics

DOI:
[10.1088/1367-2630/18/6/065002](https://doi.org/10.1088/1367-2630/18/6/065002)

Publication date:
2016

Document version
Publisher's PDF, also known as Version of record

Citation for published version (APA):
Schechter, M., Gangardt, D. M., & Kamenev, A. (2016). Quantum impurities: from mobile Josephson junctions to depletions. *New Journal of Physics*, 18, [065002]. <https://doi.org/10.1088/1367-2630/18/6/065002>

Quantum impurities: from mobile Josephson junctions to depletions

This content has been downloaded from IOPscience. Please scroll down to see the full text.

2016 New J. Phys. 18 065002

(<http://iopscience.iop.org/1367-2630/18/6/065002>)

View [the table of contents for this issue](#), or go to the [journal homepage](#) for more

Download details:

IP Address: 130.225.212.4

This content was downloaded on 19/08/2016 at 12:44

Please note that [terms and conditions apply](#).

You may also be interested in:

[Dark-soliton-like excitations in the Yang–Gaudin gas of attractively interacting fermions](#)

Sophie S Shailov and Joachim Brand

[The physics of dipolar bosonic quantum gases](#)

T Lahaye, C Menotti, L Santos et al.

[Quantum states of dark solitons in the 1D Bose gas](#)

Jun Sato, Rina Kanamoto, Eriko Kaminishi et al.

[Strongly correlated quantum fluids: ultracold quantum gases, quantum chromodynamic plasmas and holographic duality](#)

Allan Adams, Lincoln D Carr, Thomas Schäfer et al.

[Recent developments in quantum Monte Carlo simulations with applications for cold gases](#)

Lode Pollet

[Polarons, dressed molecules and itinerant ferromagnetism in ultracold Fermi gases](#)

Pietro Massignan, Matteo Zaccanti and Georg M Bruun

[Light-induced gauge fields for ultracold atoms](#)

N Goldman, G Juzelinis, P Öhberg et al.



PAPER

Quantum impurities: from mobile Josephson junctions to depletons

Michael Schecter^{1,5}, Dimitri M Gangardt² and Alex Kamenev^{3,4}¹ Center for Quantum Devices and Niels Bohr International Academy, Niels Bohr Institute, University of Copenhagen, DK-2100 Copenhagen, Denmark² School of Physics and Astronomy, University of Birmingham, B15 2TT, UK³ School of Physics and Astronomy, University of Minnesota, Minneapolis, MN 55455, USA⁴ William I Fine Theoretical Physics Institute, University of Minnesota, Minneapolis, MN 55455, USA⁵ Author to whom any correspondence should be addressed.E-mail: schecter@nbi.ku.dk**Keywords:** mobile impurity, 1D quantum liquids, Bloch oscillations, ultracold atoms, superfluidityRECEIVED
30 December 2015REVISED
10 May 2016ACCEPTED FOR PUBLICATION
12 May 2016PUBLISHED
31 May 2016Original content from this
work may be used under
the terms of the [Creative
Commons Attribution 3.0
licence](#).Any further distribution of
this work must maintain
attribution to the
author(s) and the title of
the work, journal citation
and DOI.**Abstract**

We overview the main features of mobile impurities moving in one-dimensional superfluid backgrounds by modeling it as a mobile Josephson junction, which leads naturally to the periodic dispersion of the impurity. The dissipation processes, such as radiative friction and quantum viscosity, are shown to result from the interaction of the collective phase difference with the background phonons. We develop a more realistic depletion model of an impurity-hole bound state that provides a number of exact results interpolating between the semiclassical weakly interacting picture and the strongly interacting Tonks–Girardeau regime. We also discuss the physics of a trapped impurity, relevant to current experiments with ultra cold atoms.

1. Introduction

The motion of mobile impurities in superfluid environments is a fascinating subject with a long history. The field first came to prominence in the late forties with experiments on ^4He – ^3He mixtures. It was noticed that the super flow through the supra-surface film does not involve He^3 , leading to a substantial purification of ^4He leaking out of the container [1]. The phenomenon was initially attributed to the absence of superfluidity in ^3He . Soon after, Landau and Pomeranchuk [2] realized that the effect has actually nothing to do with the quantum statistics of the impurities, but rather with the fact that foreign atoms cannot exchange energy and momentum with the superfluid fraction. Instead, the rare impurities ought to contribute to the normal fluid fraction. The nature of their interactions with the normal fraction was not elucidated in the initial 1948 short paper [2], and was dealt with in subsequent publications of Landau and Khalatnikov [3, 4] and Khalatnikov and Zharkov [5]. The latter authors realized that at small temperatures the dominant interaction process is two phonon scattering by ^3He atoms, leading to impurity diffusion and equilibration with the normal fraction. Since the scattering mechanism relies on the absorption of thermal phonons, the diffusion coefficient is sharply divergent at small temperature, T , and the corresponding linear in velocity, V , viscous friction force scales as $F_{\text{fr}} \sim T^8 V$. The theory was further developed in a number of influential papers [6–10] and verified experimentally through precision measurements of the velocity and attenuation of sound [11]. The subject was revived in the seventies in the context of the storage of cold neutrons in superfluid ^4He [12–14].

Recently the field has received growing attention due to advances in cold atom experiments. Through a number of techniques it became possible to place various impurity atoms in Bose–Einstein condensates (BEC) of alkali atoms, manipulate their mutual scattering strength and apply forces selectively to the impurity atoms. The Cambridge group [15] has used microwave pulses to flip the hyperfine state of a few spatially localized atoms in the BEC of magnetically levitated ^{87}Rb , turning them into mobile impurities. The impurities, created in the hyperfine $m_F = 0$ state, were then accelerated through the BEC by the gravitational force, not compensated by

the magnetic trap. The Innsbruck [16] and Bonn [17] groups have placed ^{133}Cs impurities in a BEC of ^{87}Rb , and magnetically tuned their mutual scattering length with a Feshbach resonance. The Florence group [18] created mixtures of ^{41}K and ^{87}Rb , and manipulated the two components with species-selective optical potentials. Another line of research [19–21] deals with inserting a single *ion* into a BEC of neutral atoms using a linear Paul trap to control the ion and study the mutual ion–atom interaction. Although at the moment the ion micromotion leads to a continuous depletion of BEC atoms from the trap [19, 21], this setup offers a potential benefit in terms of easy manipulations with the help of electrostatic fields.

One of the great advantages of the modern ultra cold atomic experiments is the control over their dimensionality by placing atoms into one, two or three-dimensional optical lattices. In particular, it has become possible to study impurity dynamics in a one-dimensional (1D) atomic background, where the transverse motion is fully quantized and only the lowest transverse sub-band is occupied by the atoms [15, 18, 22]. The peculiarity of the 1D setup is that every impurity atom effectively ‘cuts’ the host liquid, creating an effective tunneling Josephson junction (JJ) between the two superfluids. Unlike a conventional JJ, however, the impurity is mobile and is characterized by its coordinate and momentum, in addition to the Josephson phase, Φ , across it. As we explain below, the Josephson physics (and in particular the periodic dependence of energy on Φ) leads to a *qualitative* change of the impurity dispersion relation, which goes far beyond a simple mass renormalization usually considered in higher dimensions. The actual energy-momentum relation $E(P, n)$ of a mobile impurity in a 1D superfluid with density n is a *periodic* function of the total momentum P with the period $2\pi\hbar n$. This periodicity is due to the fact that in a system of size L with nL particles, the momentum $nL \times (2\pi/L) = 2\pi n$ may be transferred to the 1D Galilean invariant host liquid with the energy cost $nL \times (2\pi/L)^2/(2m)$, negligible in the $L \rightarrow \infty$ limit (here and below we set $\hbar = 1$ and m is the atomic mass of the host superfluid). Therefore, the groundstate of a large system whose momentum is an integer multiple of $2\pi n$ corresponds to a super-flowing host and an impurity at rest with respect to it. We note that these considerations are not applicable in dimensions larger than one.

By following the dispersion curve $E(P, n)$ adiabatically through the application of a small external force F to the impurity, one expects to see Bloch oscillations with period $2\pi n/F$ *in the absence of any periodic lattice*. The mechanism behind these oscillations, first predicted in [23], was attributed to the emergence of an effective crystalline order of the background atoms, robust against thermal fluctuations for sufficiently low temperatures as well as phonon radiation for sufficiently small external forces.

Although the dynamics of mobile impurities in 1D atomic condensates has attracted a lot of attention [23–34], a systematic pedagogical exposition of the consequences of the above mentioned periodic dispersion is still missing. This paper serves to fulfill this gap. Here we investigate the dynamics of mobile impurities in a 1D quantum liquid, exploring similarities and differences with the Josephson physics. Our particular focus is on the conditions where the Bloch oscillations may be observed. To this end we consider the thermal friction (i.e. due to the normal fraction) along with the acceleration induced phonon radiation losses. We also put a special emphasis on the consequences of being close to exactly integrable points in the parameter space of impurity mass and impurity–host interaction strength. An amazing consequence of dealing with Galilean invariant 1D systems is that a number of exact results are available even away from such integrable points. We will show below that the dispersion relation $E(P, n)$, a *static* quantity available numerically or analytically in a number of limiting cases, determines many *dynamic* characteristics exactly, including those going beyond the linear response theory. Finally, we apply our results obtained for translationally invariant systems to the trap geometry with an external adiabatic potential. We give a number of estimates for systems whose parameters are taken from recent experiments [15, 18] as well as their immediate extensions.

The paper is organized as follows: in section 2 we illustrate the main ideas behind the physics of quantum impurities with a simple, yet a non-trivial, model of a moving Josephson Junction (mJJ). In section 3 we introduce the coupling of an impurity to the background modeled as an elastic medium (phonons). We discuss the mechanism of energy and momentum losses induced by such coupling and derive the expression for the mobility. The simple model is then generalized to describe the impurity dynamics in any interacting quantum liquid at the expense of introducing an additional coupling to density fluctuations in section 4. We illustrate this formalism in section 5 by deriving our previous results for the impurity dynamics in a weakly interacting background. We then consider the background consisting of impenetrable bosons (the Tonks–Girardeau (TG) gas) where the impurity becomes a heavy polaron. We derive the first main result of the paper for the mobility of heavy polarons in section 6. The second main result corresponds to the description of impurities in a harmonically trapped background and is presented in section 7. We conclude and discuss open questions in section 8.

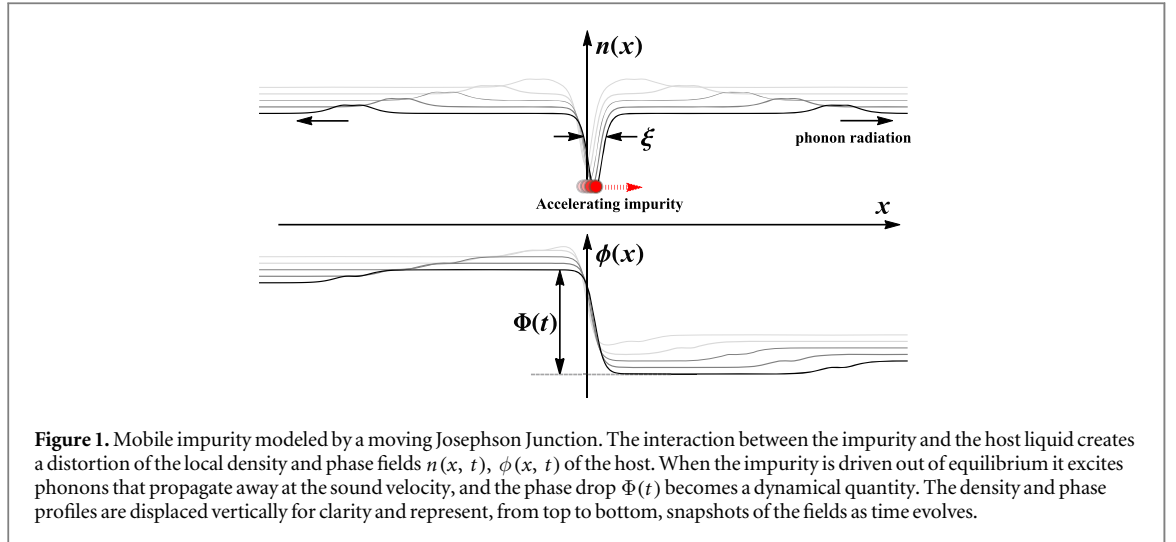


Figure 1. Mobile impurity modeled by a moving Josephson Junction. The interaction between the impurity and the host liquid creates a distortion of the local density and phase fields $n(x, t)$, $\phi(x, t)$ of the host. When the impurity is driven out of equilibrium it excites phonons that propagate away at the sound velocity, and the phase drop $\Phi(t)$ becomes a dynamical quantity. The density and phase profiles are displaced vertically for clarity and represent, from top to bottom, snapshots of the fields as time evolves.

2. Moving Josephson junction model

The essential physics of a mobile impurity is most easily illustrated by a strongly repulsive impurity moving in a background of weakly interacting bosons. It can be modeled by a weak link located at the position X separating two condensates⁶. The phase difference Φ between the two condensates, figure 1, gives rise to the Josephson term in the energy

$$H_d(\Phi) = -nV_c \cos \Phi + \mu N, \quad (1)$$

The critical velocity, denoted by V_c , is defined as the maximal slope of the dispersion $\partial E / \partial P$ at fixed density n , and depends on the impurity-background interaction. The last term in equation (1) takes into account the number of particles N depleted by the impurity. Here we are working in the grand-canonical ensemble with the chemical potential $\mu \approx gn$ fixed by the background density n and interaction parameter g .

The phase drop Φ inevitably creates a small background supercurrent $n\Phi/mL$. While the contribution of the supercurrent to the total energy is of the order of $1/L$, its contribution to the total momentum P is independent of the system size, and is given by $n\Phi$. The total energy of the mJJ is thus the combination of the Josephson term, equation (1) and the kinetic energy of the localized impurity

$$H(P, X, \Phi) = \frac{1}{2\mathcal{M}}(P - n\Phi)^2 + U(X) + H_d(\Phi). \quad (2)$$

where $\mathcal{M} = M - mN$ is the total mass of the impurity, including the mass of N particles it depletes from its vicinity. We have also included an external potential $U(X)$, e.g. of gravitational or optical origin, acting on the impurity.

The phase drop Φ represents a collective coordinate characterizing the state of the impurity's depletion cloud. In equilibrium its value is determined from the requirement of the minimum of the total energy (2):

$$(P - n\Phi)/\mathcal{M} = V_c \sin \Phi. \quad (3)$$

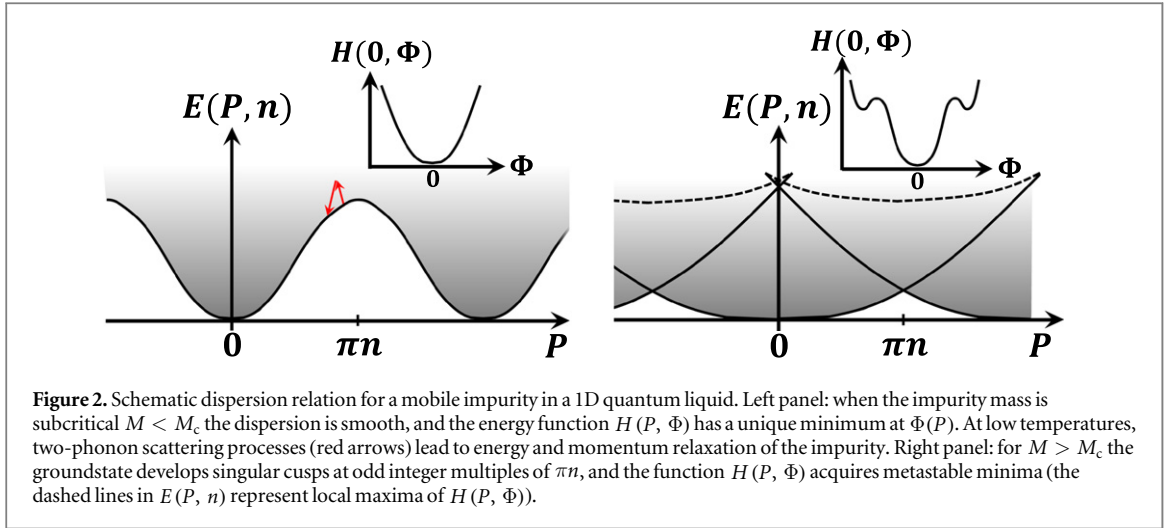
The physical meaning of this condition is the matching between the current $I = nV$ of the background particles moving with velocity $V = (P - n\Phi)/\mathcal{M}$ across mJJ and the Josephson current $nV_c \sin \Phi$. Equation (3) admits a solution $\Phi(P, n)$ that may be substituted into the Hamiltonian (2) to obtain the dispersion curve $H(P, \Phi(P, n)) = E(P, n)$ of the mJJ in the absence of the external potential U . Using the minimum condition equation (3) one may show that the velocity of the impurity satisfies

$$V = (P - n\Phi)/\mathcal{M} = \partial E / \partial P, \quad (4)$$

which defines the group velocity of the impurity dressed by the depletion cloud.

One may notice a close similarity of the mobile impurity Hamiltonian (2) and the SQUID or phase qubit [35]. In this analogy n^2/\mathcal{M} plays the role of the inductance of the SQUID loop, while the dimensional ratio P/n is a direct analog of the external flux (in units of the flux quantum), permeating the loop. As in the case of the SQUID, the thermodynamic quantities are periodic functions of the external flux with the period 2π , implying the periodicity of the dispersion relation $E(P + 2\pi n, n) = E(P, n)$, see figure 2. For example, in the case of a

⁶ According to the Bogoliubov–Mermin–Wagner theorem the true condensate is absent in one spatial dimension. Nevertheless, for our purposes the existence of a *local* superfluid order is sufficient to define the phase difference across the impurity.



strong repulsive impurity, $V_c \ll c$, we have from equation (3): $\Phi(P, n) \approx P/n$ and $E(P, n) \approx -nV_c \cos(P/n) + \mu N$.

Periodicity of the impurity's energy-momentum relation has dramatic consequences for its dynamics: if the momentum is linearly increased $P = Ft$ by an external force $F = -\partial_X U$, the velocity of the impurity does not increase indefinitely but changes *periodically*, exhibiting Bloch oscillations with the period $\tau_B = 2\pi n/F$, [23, 25]. This spectacular phenomenon is a close relative of the AC Josephson effect: under an applied constant force (voltage), the impurity velocity (current) is an oscillatory function of time. The mechanism is that once the time-dependent phase shift $\Phi(t)$ reaches π , the system undergoes a phase slip from $\pi \rightarrow -\pi$, which channels momentum $2\pi n$ into the superfluid background flow, and reverses the direction of the impurity's motion.

Another useful analogy is that of an impurity propagating in a periodic potential with the period n^{-1} (this would be the case if the host gas forms a rigid 1D crystal). The energy spectrum of the impurity in such a lattice consists of Bloch bands periodic across the Brillouin zone with the width $2\pi n$. Despite the fact that the background liquid is not actually a lattice, the *groundstate* energy of the liquid with an impurity is nevertheless a periodic function of the *total* momentum P , analogous to the lowest Bloch band in a periodic potential. The difference is that in the liquid there is a continuum of gapless excitations above the groundstate $E(P, n)$, which are due to the presence of the phononic modes. In the case of the rigid lattice, excited states at fixed momentum are separated by an energy gap, so the leading deviation from adiabaticity in the presence of an external force is given by exponentially weak Landau-Zener tunneling processes. The gapless modes of the superfluid background modify the adiabatic picture of Bloch oscillations in a much more substantial way. To capture the dynamics of a driven impurity we must generalize the static picture to the situation where Φ is a *dynamical* variable. This is achieved in the next section by introducing the coupling of the impurity to phonons.

We mention that equation (3) may admit several distinct solutions for some range of momentum P when the impurity mass M exceeds a critical value M_c (i.e. for $MV_c/n > 1$). This corresponds to multiple metastable minima of the function $H(P, \Phi)$, which, for the case of a SQUID, represent trapped flux states in a system with large inductance. From equations (2) and (3) one can see that for $M > n/V_c$ there are two exactly degenerate groundstates when the momentum is an odd multiple of πn (these two states reflect the two distinct solutions for $\Phi(P = \pi n)$). By changing the momentum P across such a point the relative position of the two minima interchange, leading to a discontinuous jump of $\Phi(P)$. This leads to a cusp in the dispersion relation $E(P)$, figure 2, which for bosonic gases (with $K > 1$, see below) is not smeared by quantum fluctuations for sufficiently weak impurity-host coupling ($G < G_c$), as was first realized in [36]. This is consistent with the notion of critical mass discussed above, since the critical coupling G_c is dependent on the impurity mass M (and the critical mass is coupling dependent). The specific dependence of G_c on system parameters (e.g. M) was not discussed in [36]. Since $M_c(G \rightarrow 0) > 0$ is finite, we find that $G_c = 0$ when $M < M_c(G \rightarrow 0)$ (i.e. the cusp is absent for any $G > 0$). The critical mass $M_c(G \rightarrow 0)$ depends only on the Luttinger parameter of the gas, and diverges in the limits $K \rightarrow 1$ and $K \rightarrow \infty$, where the cusp is known to be absent for any $M < \infty$. When it exists, the cusp leads to qualitative changes in the dynamics of a driven impurity due to the 'overshooting' of the groundstate branch of the dispersion, and was discussed in [26].

Another remarkable phenomenon is the macroscopic quantum tunneling of phase between successive minima of $H(P, \Phi)$ [37]. It leads to the possibility of an impurity, trapped in such a meta-stable state, to transfer its energy and momentum to the host and thus experience an effective friction force F_{fr} even at zero temperature. Such a friction force appears to be a highly nonlinear function of the impurity velocity [38, 39]. It may seem to contradict the notion, discussed in the introduction, that only the normal fraction exerts friction on the

impurity. The reason is that the condensate is, strictly speaking, absent in 1D even at $T = 0$ due to long wavelength fluctuations of the phase. Moreover, once a heavy impurity reaches the lowest minimum of $H(P, \Phi)$ it moves indefinitely (super flows) with a small velocity up to $\sim \pi n/M$, without any friction at $T = 0$. A light impurity, $MV_c/n < 1$, does not exhibit metastable minima and is bound to relax to its only stable minimum $E(P, n)$, where it does *not* experience any $T = 0$ friction, linear or nonlinear.

Another frequent misconception associated with a light mobile impurity, as opposed to a static impurity or a tunneling barrier, is the interaction-induced renormalization of its tunneling transparency. To make an extreme version of the argument, consider an impurity in a repulsively interacting Fermi gas. According to Kane and Fisher [40] the tunneling transparency renormalizes to zero in the limit of zero temperature, independent of the initial bare value. This seemingly suggests that such an impenetrable impurity cannot move and its dispersion must be flat. The flaw in this argument is that the Kane–Fisher renormalization is based on the $2k_F = 2\pi n$ backscattering processes, which for a finite mass impurity are associated with the recoil energy $E_R = (2\pi n)^2/(2M)$. The renormalization thus terminates at this finite energy scale [41], leaving the tunneling transparency and dispersion bandwidth finite. As a result, a finite mass impurity has a non-flat ($2\pi n$ periodic) dispersion relation $E(P, n)$ even in a repulsive Fermi gas.

Below, we focus on the experimentally most relevant case, where the mass is subcritical and the dispersion is a smooth periodic function of momentum, while $H(P, \Phi)$ has a unique stable minimum at $\Phi = \Phi(P, n)$. For the case of impurities with a supercritical mass we refer the reader to [26].

3. Impurity-phonon coupling and dissipation

The static picture of the previous section needs to be modified if the Josephson phase Φ becomes time-dependent. Since instantaneous changes of the phase in the left/right condensates are impossible, one must take into account the generated gradients of the phase field, i.e. local currents which, in turn, lead to the density transport in the form of phononic excitations, as illustrated in figure 1.

For nonzero phononic fields, the impurity is subject to the modified local supercurrent. The Josephson Hamiltonian (1) should be modified by the tilting term

$$H_{\text{int}} = -\delta I \Phi, \quad (5)$$

where $\delta I = (\delta \dot{N}_L - \delta \dot{N}_R)/2$ is the current through the impurity, given by the rate of change of the excess number of particles to the left, δN_L , and to the right, δN_R , of the impurity. Expressing these numbers via the integral of the density field

$$\delta N_L = -\delta N_R = \int_{-\infty}^X \rho(x, t) dx = \frac{1}{\pi} \vartheta(X, t), \quad (6)$$

and using the standard bosonization definition [42] $\rho = \partial_x \vartheta / \pi$ of the field $\vartheta(x, t)$, we obtain

$$H_{\text{int}} = -\frac{1}{\pi} \Phi \frac{d}{dt} \vartheta(X, t) = \frac{1}{\pi} \dot{\Phi}(t) \vartheta(X, t), \quad (7)$$

where the full time derivative was omitted. Obviously, this term is only relevant for a time-dependent Josephson phase $\dot{\Phi} \neq 0$. Notice that it does not involve any coupling constants and thus represents a universal coupling of the collective variable Φ to the phononic degrees of freedom described by the field $\vartheta(x, t)$ and its canonical conjugate superfluid phase field $\varphi(x, t)$. Their dynamics can be linearized near equilibrium, resulting in the Luttinger liquid Hamiltonian [42]

$$H_{\text{ph}} = \frac{c}{2\pi} \int dx \left[\frac{1}{K} (\partial_x \vartheta)^2 + K (\partial_x \varphi)^2 \right]. \quad (8)$$

Here $K = \pi n/mc$ is the Luttinger parameter, proportional to the compressibility of the background liquid. For a weakly interacting superfluid $K \gg 1$, while for impenetrable bosons $K = 1$.

We now integrate out the phononic degrees of freedom using the Keldysh technique [43] as explained in [25]. As a result we obtain a quantum dissipative action, similar to that of the Caldeira–Leggett model [37]. The dissipation arises naturally from the continuous spectrum of phonons with a constant density of states at small energy, described by equation (8). This procedure results in a generically time non-local effective action for the impurity degrees of freedom $X(t)$ and $P(t)$, coupled to the collective variable $\Phi(t)$.

3.1. Zero-temperature dynamics and nonlinear mobility

Postponing a discussion of fluctuation effects until section 3.2, we focus here on the deterministic part of the corresponding equations of motion, which are obtained by variation of the effective action with respect to the ‘quantum’ components [25] of $\Phi(t)$ and $X(t)$ degrees of freedom. The phase variable exhibits over-damped dynamics with the effective ‘friction’ coefficient $K/2\pi$,

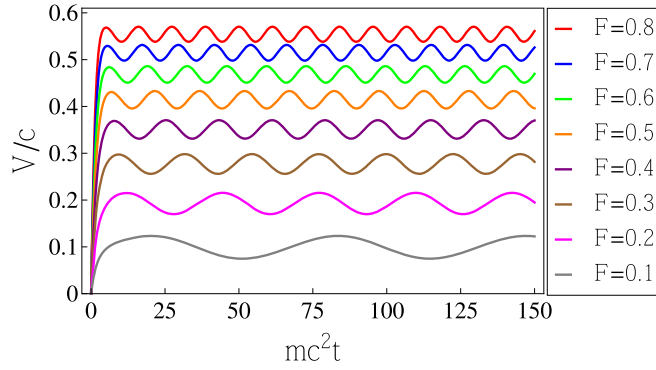


Figure 3. Schematic velocity as a function of time for various forces listed in the legend (F in units of $F_{\max} = 2nmc^2$). As F increases, the drift velocity and frequency of oscillations increases.

$$\frac{K}{2\pi} \dot{\Phi} = -\frac{\partial H}{\partial \Phi}, \quad (9)$$

where the Hamiltonian H is given by equation (2). If the initial phase drop is off-equilibrium, it will evolve towards the value which minimizes H by radiating away the excess phase difference in the form of phonons, see figure 1. This results in an energy loss with the instantaneous rate

$$W = \frac{\partial H}{\partial \Phi} \dot{\Phi} = -\frac{K}{2\pi} \dot{\Phi}^2. \quad (10)$$

In addition to the energy loss, the radiation of phonons also leads to the loss of momentum, i.e. a radiation friction force, F_{rad} . The equation for the momentum for the mobile impurity becomes

$$\dot{P} = F + F_{\text{rad}} = -\frac{\partial U}{\partial X} - \frac{K}{2\pi} \frac{V}{c^2} \dot{\Phi}^2. \quad (11)$$

The main effects of the energy and momentum losses are to renormalize the period of oscillations τ_B and to introduce a finite drift velocity V_D , [25]. The latter can be obtained from calculating the power radiated to the phononic bath averaged over one period of oscillations and equating it to the work done by the external force:

$$FV_D = -\langle W \rangle_{\tau_B} = -\frac{1}{\tau_B} \int_0^{\tau_B} \frac{K}{2\pi} \dot{\Phi}^2 dt. \quad (12)$$

Using $\dot{\Phi} = (\partial \Phi / \partial P) \dot{P}$ and $\dot{P} \approx F$, we see that the drift velocity is proportional to the external force $V_D = \sigma F$. The proportionality coefficient is the *nonlinear* mobility σ , given by the integral over the Bloch oscillation period

$$\sigma = \frac{1}{2\pi n} \int_0^{2\pi n} \frac{K}{2\pi} \left(\frac{\partial \Phi}{\partial P} \right)^2 dP \approx \frac{K}{2\pi n^2}, \quad (13)$$

where the last approximate equality is obtained assuming that $\Phi \approx P/n$. This result can be interpreted as an inverse resistance using the analogy with electrical current: in the co-moving frame the impurity experiences current $I = nV_D$ and the power dissipated on the impurity should be supplied by the external force, $I^2 R = FV_D$, hence $1/R = n^2 \sigma = K/2\pi$. It is exactly the electrical resistance of a clean Luttinger liquid [42], $R = \hbar/e^2 K$, if one uses units such that $\hbar = e = 1$.

By no means should equation (13) be interpreted in terms of linear response theory: the drift motion of the impurity is superimposed with the nonlinear Bloch oscillations, see figure 3. The modified period of the oscillations can be calculated from the relation

$$2\pi n = \int_0^{\tau_B} \dot{P} dt = \tau_B (F - \langle F_{\text{rad}} \rangle_{\tau_B}). \quad (14)$$

Using $\langle F_{\text{rad}} \rangle_{\tau_B} / F \approx \sigma^2 F^2 / c^2$ we obtain the renormalized period

$$\tau_B = \frac{2\pi n}{F} \frac{1}{1 - (F/F_{\max})^2}. \quad (15)$$

⁷ The inverse proportionality to the Luttinger parameter is consistent with the fact that the ‘wire’ length is infinite and the effects of the ‘leads’ discussed in [61] are irrelevant in our case.

Table 1. Maximal force and critical densities related to observing Bloch oscillations of an impurity created in the $m_F = 0$ hyperfine state for various quantum gases with typical gas parameters. Top row: ratio of the maximal force over the gravitational force assuming a density of background particles $n = 0.65 \mu\text{m}^{-3}$ in the strong coupling regime $\gamma \approx 7$ (as used in [15] for Rb) where $F_{\text{max}} \approx 8n^3/m$. At this density, Bloch oscillations are expected to occur for Li and Na, corresponding to $F_{\text{max}}/F_{\text{grav}} > 1$ (bold entries). Bottom row: critical density of various gases at fixed coupling $\gamma = 7$. For $n > n_{\text{crit}}$ Bloch oscillations are expected to occur.

	Li	Na	K	Rb	Cs
$F_{\text{max}}/F_{\text{grav}}$	25	1.7	0.54	0.12	0.05
$n_{\text{crit}} (\mu\text{m}^{-3})$	0.22	0.55	0.80	1.32	1.75

This expression can be trusted only for small forces $F \lesssim F_{\text{max}}$, where the characteristic force F_{max} is given by

$$F_{\text{max}} = \frac{c}{\sigma} \approx 2mc^2n. \quad (16)$$

Beyond this characteristic force the drift velocity exceeds the speed of sound c and impurity emits Cherenkov radiation of phonons, which dramatically increases its energy and momentum losses. Since the Bloch oscillations do not take place in this regime, we shall not discuss it here.

We note that for the experiment of [15], which used two hyperfine states of ^{87}Rb for the impurities and background gas, the coupling is rather strong $mg/n \sim 7$. In this case the mobility is close to $\sigma = K/2\pi n^2 \approx 1/2\pi n^2$. The external force is provided by the gravitational field, which gives a drift velocity $V_D/c \sim 8$. The gravitational force thus exceeds the maximal force $F_{\text{max}} = 2\pi^2 n^3/m$ by a factor of 8, and our low-energy theory is inapplicable. The Bloch oscillations do not occur, and instead the impurities become supersonic before exiting the gas. However, owing to the strong density dependence of F_{max} , a gas twice as dense (or sufficiently lighter, e.g. Li and Na) would provide a maximal force comparable to the gravitational one and Bloch oscillations become possible, see table 1. The crossover between strong and weak force at $F = F_{\text{max}}$ was studied numerically and reported in the arXiv version of [28]. These results are qualitatively consistent with our theoretical predictions.

3.2. Fluctuations

So far we have considered the zero temperature dynamics of an accelerated impurity. We turn now to the finite temperature regime and focus on the thermal fluctuations of the host liquid. In doing so we shall assume that the liquid is at thermal equilibrium with temperature T in the laboratory reference frame, and thus acts as a bath for the impurity. In a generic (non-integrable) case one expects that an excited impurity should thermalize by losing its excess energy and momentum to the bath in the form of phonon emission.

The problem, however, is that due to the velocity mismatch, $V < c$, the emission of a single phonon is energetically forbidden since $|E(P, n) - E(P \pm \omega/c, n)| < \omega$ (here \pm refers absorption of a right/left moving phonon with energy ω). The leading process of energy and momentum exchange is therefore the *two-phonon* process. In this case the impurity first absorbs a thermal phonon with energy $\omega \approx T$, bringing it to the virtual state with momentum $P \pm \omega/c$, and then emits a Doppler shifted phonon with the energy $\omega_{\pm} \approx \frac{c \mp V}{c \pm V} \omega$, see figure 2. One notices that, while both processes happen at the same rate, there is a net momentum loss between them in the amount $(\omega_- - \omega_+)/c \propto V\omega/(c^2 - V^2)$. At small velocity $V \ll c$, this implies a linear in velocity thermal friction force

$$F_{\text{fr}} = -\kappa(T)V \quad (17)$$

acting on the impurity.

The above considerations indicate that: (i) since the two-phonon process relies on thermal phonons, the friction coefficient $\kappa(T)$ is strongly temperature dependent and vanishes at $T = 0$; (ii) the thermalization process is not uni-directional, but is rather diffusive with a drift in the momentum space. Indeed, the same procedure of integrating out the phonons, described in section 3, leads naturally to the additional stochastic terms in the equations of motion. They originate from the parts of the action that are quadratic in the ‘quantum’ Keldysh components of the fields $\vartheta(X, t)$ and $\varphi(X, t)$, evaluated at the impurity coordinate. These fields can be conveniently decomposed into two independent (chiral) auxiliary fields $\xi_{\pm}(t)$, whose equilibrium correlation functions

Table 2. Ratio of the minimal force over the gravitational force and mobilities for various quantum gases with typical gas parameters. We assume the impurity is created in a distinct hyperfine state of the gas with the impurity-gas scattering length differing from the gas-gas scattering length by 10% (when they are equal, or if the background gas is in the Tonks–Girardeau limit $F_{\min} = 0$, $\sigma_{\text{Kubo}} = \infty$ due to integrability). In all cases we have assumed a temperature $T = 0.5mc^2$, density $n = 0.65 \mu\text{m}^{-1}$ and coupling strength $\gamma = 7$. Due to the closeness to integrability, the gravitational force always greatly exceeds the minimal force, and gives rise to Bloch oscillations if $F_{\text{grav}} < F_{\max}$ (see table 1).

	Li	Na	K	Rb	Cs
$F_{\min}/F_{\text{grav}} [\times 10^{-5}]$	7.4	0.69	0.22	0.05	0.02
$\sigma [\mu\text{m}^2/\hbar]$	2.4	2.4	2.4	2.4	2.4
$\sigma_{\text{Kubo}} [\mu\text{m}^2/\hbar \times 10^3]$	1.5	1.5	1.5	1.5	1.5

$$\langle \xi_{\pm}(\omega) \xi_{\pm}(-\omega) \rangle = K\omega \coth \frac{\omega}{2T_{\pm}} \quad (18)$$

depend on the Doppler-shifted temperature $T_{\pm} = T(1 \mp V/c)$. The corresponding equations of motions for the phase $\Phi(t)$ and momentum $P(t)$ are modified to become

$$\frac{K}{2\pi} \dot{\Phi} = -\frac{\partial H}{\partial \Phi} + (\xi_+ + \xi_-), \quad (19)$$

$$\dot{P} = F - \frac{K}{2\pi} \frac{V}{c^2} \dot{\Phi}^2 + \frac{1}{c} \dot{\Phi}(\xi_+ - \xi_-). \quad (20)$$

Notice that, since the impurity interacts with the liquid through the time dependent phase shift, equation (7), the stochastic term in its equation of motion also comes with the multiplicative $\dot{\Phi}$ factor, understood in the sense of Ito calculus. The friction force, due to the two-phonon processes discussed above, may be obtained from equations (19) and (20) as follows. We solve equation (19) as a frequency (time-derivative) expansion as $K\dot{\Phi}/2\pi = -\frac{\Gamma}{2}(\xi_+ + \xi_-) - \frac{\Gamma^2}{4}(\ddot{\xi}_+ + \ddot{\xi}_-) + \dots$, where $\Gamma^{-1} = -(\pi/K)\partial_{\Phi}^2 H$, or according to equation (2), $\Gamma \approx -K\mathcal{M}/\pi n^2$. Substituting this expansion into the last term of equation (20) and averaging over the noise according to equation (18), one finds to the leading order in V/c

$$F_{\text{fr}} = \frac{\pi\Gamma^2}{2Kc} [\langle \xi_+ \ddot{\xi}_+ \rangle - \langle \xi_- \ddot{\xi}_- \rangle] \simeq -\frac{\Gamma^2}{4c} \int_0^{\infty} \frac{d\omega}{2\pi} \frac{\omega^4}{\sinh^2 \frac{\omega}{2T}} \frac{V}{cT} = -\frac{2\pi^3}{15c^2} \Gamma^2 T^4 V. \quad (21)$$

As a result the friction coefficient in equation (17) is given by

$$\kappa(T) = \frac{2\pi^3}{15c^2} \Gamma^2 T^4. \quad (22)$$

The T^4 dependence of the friction coefficient in 1D, at low temperatures, was first found by Castro-Neto and Fisher [41]. This result is a 1D generalization of 3D Khalatnikov's T^8 result [3–10], mentioned in the Introduction. We will show below that, beyond the simple model discussed here, the amplitude Γ may be expressed *exactly* in terms of the impurity dispersion relation $E(P, n)$. One can then check explicitly that for all known exactly solvable models $\Gamma = 0$ [52], consistent with the idea that integrable systems do not thermalize.

At finite temperature we therefore have two distinct regimes: for $F < F_{\min} = \kappa(T) V_c$ Bloch oscillations do not occur and after some initial acceleration the impurity attains a steady state with the drift velocity $V_D = F/\kappa(T) = \sigma_{\text{Kubo}} F$. In the low temperature regime considered here, the linear Kubo mobility $\sigma_{\text{Kubo}} \gg \sigma$ is large, see table 2. In the range $F_{\min} < F < F_{\max}$, Bloch oscillations appear with the renormalized period $\tau_B = 2\pi n / \sqrt{F^2 - F_{\min}^2}$, while the corresponding drift velocity is approximately given by $V_D \approx \sigma F + \sigma_{\text{Kubo}} F_{\min}^2 / 2F$. As a result, the drift velocity is a non-monotonous function of the applied force with a sharp local maximum $V_D \approx V_c$ at $F \approx F_{\min}$. Alternatively at a fixed force, the drift velocity is a non-monotonous function of temperature with a maximum attained when $\kappa(T) = F/V_c$.

An additional consequence of the noise terms in equations (19) and (20) is dephasing of the oscillations even at zero temperature due to quantum fluctuations. Using the last term in equation (20), together with $\Phi \approx P/n$, we have

$$\Phi(t) \simeq \frac{1}{n} \int_0^t dt' \dot{P}(t') \simeq \frac{F}{n} \left[t + \frac{1}{c} \int_0^t dt' (\xi_+ - \xi_-) \right]. \quad (23)$$

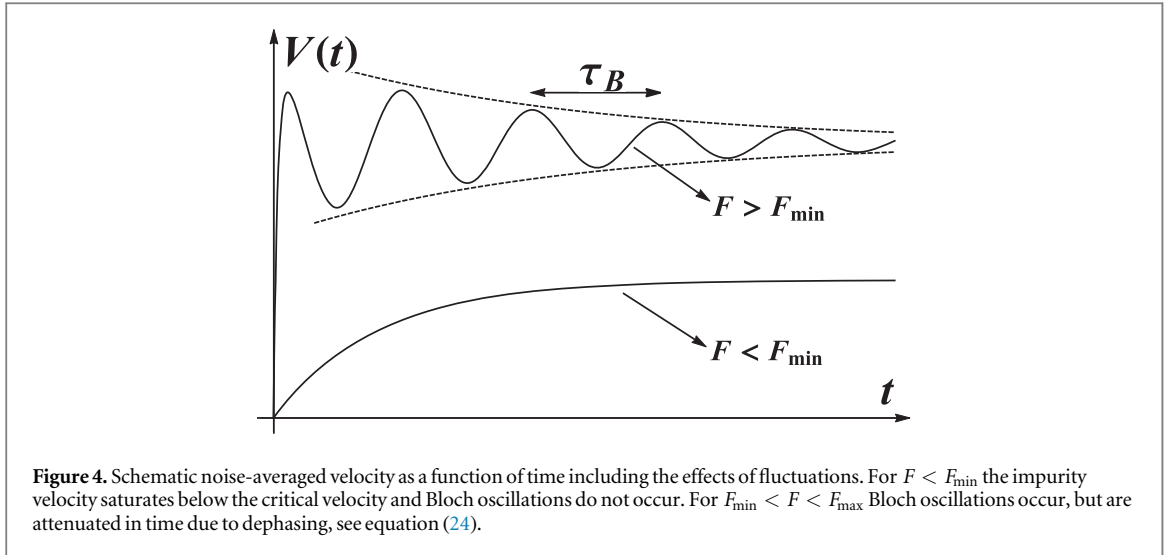


Figure 4. Schematic noise-averaged velocity as a function of time including the effects of fluctuations. For $F < F_{\min}$ the impurity velocity saturates below the critical velocity and Bloch oscillations do not occur. For $F_{\min} < F < F_{\max}$ Bloch oscillations occur, but are attenuated in time due to dephasing, see equation (24).

As a result, the oscillatory part of the noise-averaged velocity decays as a power law at long times $\mu t > 1$:

$$\langle V(t) \rangle = V_D + V_c \langle \sin \Phi(t) \rangle = V_D + \frac{V_c}{(\mu t)^\alpha} \sin \frac{Ft}{n}, \quad (24)$$

where $\alpha = (4\pi/K)(F/F_{\max})^2$. The behavior of the impurity velocity is illustrated in figure 4. At finite temperature the same calculation results in the exponential decay for the envelope of the Bloch oscillations: $\langle V(t) \rangle \approx V_D + V_c \sin(Ft/n) \left(\frac{\pi T / \mu}{\sinh(\pi T t)} \right)^\alpha$, which may lead to complete blurring of Bloch oscillation phenomenon, in contrast to the power law dephasing at $T = 0$.

4. Mobile impurity in a generic superfluid background: the depletion model

The phenomenology and the formalism, outlined above, are in no way restricted to the mJJ model. The generic description is obtained by acknowledging that in addition to the phase $\Phi(t)$ there is another collective degree of freedom, which may be chosen as the number of depleted particles $N(t)$. The presence of two slow collective variables follows from the presence of two conservation laws: momentum and particle number. For a system conditioned to fixed values of Φ and N , all other degrees of freedom equilibrate quickly on the timescale μ^{-1} to form an optimal depletion cloud. On the other hand, changing Φ and N is only possible by channeling momentum and particles into excitations of the liquid. When the time variation of Φ , N is slow (e.g. due to a small external force), these excitations consist of soft phonons whose wavelength greatly exceed the size of the depletion cloud ξ leading to the appearance of a fast time scale ξ/c . This time scale, being compared with the period of Bloch oscillations $\tau_B = 2\pi n/F$, provides the upper bound on the external force F . This bound is identical to the previously formulated condition $F < F_{\max}$ and we use such an adiabatic approach to develop an analytically tractable theory for the low-energy impurity dynamics [25]. Recently this adiabatic approach was criticized in [30, 31, 33, 44], where the Bloch oscillations were found to be absent for a sufficiently light impurity and where, for a heavy impurity, the drift velocity was found to be much larger than the one predicted by the linear law $V_D = \sigma F$.

This critique was based on the apparent lack of adiabaticity due to the absence of the energy gap to low-energy excitations. We note here, however, that these excitations are phonons that travel quickly away from the depleton and thus leave it in a state of local equilibrium, sufficient for using the concept of adiabaticity. In our approach the adiabaticity (in the sense of depleton being close to its instantaneous ground-state) is assumed and then proven self-consistently by calculating the energy and momentum transferred to the host liquid, leading naturally to the upper bound on the external force equation (16).

The Hamiltonian (2) is generalized to

$$H(P, X, \Phi, N) = \frac{1}{2} \frac{(P - n\Phi)^2}{M - mN} + U(X) + \mu N + H_d(\Phi, N). \quad (25)$$

The quantity $H_d(\Phi, N)$ is the so-called depleton energy and is constructed in such a way that the minimization of $H(P, \Phi, N)$ (without $U(X)$) with respect to Φ , N for fixed momentum P and density n yields the equilibrium dispersion $E(P, n)$ of the impurity. Conversely, if the exact groundstate energy $E(P, n)$ is known, $\Phi(P, n)$ and $N(P, n)$ can be determined from the partial derivatives of $E(P, n)$ by solving the equations

$$\frac{\partial E}{\partial P} = \frac{P - n\Phi}{M - mN} = V; \quad \frac{\partial E}{\partial n} = -V\Phi + \frac{mc^2}{n}N, \quad (26)$$

where the density dependence of the speed of sound $c = c(n)$ is implied. The first of equations (26) is identical to equation (4), while the second relation in equation (26) follows from taking the density partial derivative of equation (25) in equilibrium, defined by $\partial_N H = \partial_\Phi H = 0$.

The equilibrium values of $N(P, n)$, $\Phi(P, n)$ are also directly related to the edge exponents of the impurity spectral function $A(P, \omega)$, which represents the probability for an impurity with momentum P and energy ω to tunnel into the ground state of the liquid [36, 45–51]. Because $E(P, n)$ defines the lower edge of the many-body spectrum in the presence of the impurity, we have $A(P, \omega) \propto \Theta(\omega - E(P, n))[\omega - E(P, n)]^{\beta(P, n)}$, where $\beta = 2K[(\Phi/2\pi)^2 + (N/2K)^2] - 1$. The power law behavior at the spectral threshold is a consequence of the orthogonality catastrophe and was discussed extensively in the review [51] in terms of the phonon scattering phase shifts $\delta_\pm/\sqrt{\pi} = -\sqrt{K/\pi}\Phi \mp \sqrt{\pi/K}N$. These relations provide an interpretation of the phase drop Φ and the number of depleted particles N beyond the semiclassical regime of weakly interacting bosons. Indeed, the phase shifts δ_\pm of the chiral low energy excitations across a moving impurity may be defined for any interaction strength.

The coupling, equation (7), must now be generalized to include the dynamics of N . The form of the coupling remains universal and is given by

$$H_{\text{int}} = \frac{1}{\pi} \dot{\Phi} \vartheta(X, t) + \dot{N} \varphi(X, t). \quad (27)$$

Together with the Hamiltonian in equation (25) the last equation defines the depletion model. Integrating out the phononic modes leads to the coupled dynamical equations for P, X, Φ, N . Their solution in the limit $F \rightarrow 0$ yields the exact nonlinear mobility

$$\sigma = \frac{1}{2\pi n} \int_{-\pi n}^{\pi n} dP \left(\frac{c^2}{c^2 - V^2} \right) \left[\frac{K}{2\pi} \left(\frac{\partial \Phi}{\partial P} \right)^2 + \frac{V}{c} \left(\frac{\partial N}{\partial P} \right) \left(\frac{\partial \Phi}{\partial P} \right) + \frac{\pi}{2K} \left(\frac{\partial N}{\partial P} \right)^2 \right]. \quad (28)$$

For the thermal friction force one finds

$$F_{\text{fr}} = -\frac{2\pi^3}{15c^2} |\Gamma|^2 \left(\frac{c^2 + V^2}{c^2 - V^2} \right) T^4 V. \quad (29)$$

It has the same form as equation (21) with the only difference that the phononic backscattering amplitude Γ depends on derivatives of both collective variables

$$\Gamma(P, n) = -\frac{1}{c} \left(\frac{M}{m} \frac{\partial \Phi}{\partial P} + \Phi \frac{\partial N}{\partial P} - N \frac{\partial \Phi}{\partial P} + \frac{\partial N}{\partial n} \right). \quad (30)$$

As discussed below, the backscattering amplitude and therefore the thermal friction force vanish for integrable models [52].

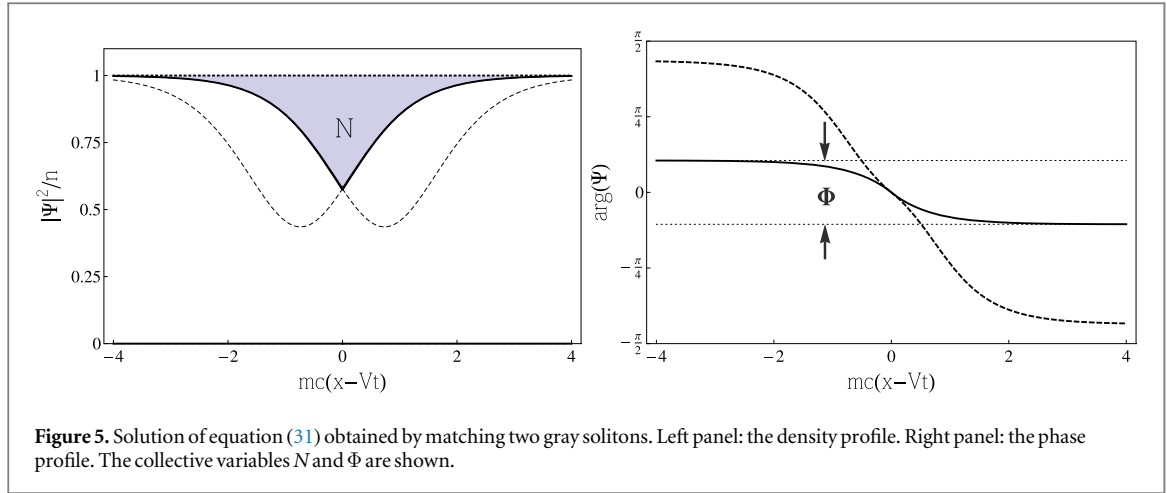
It is remarkable that finding dynamical quantities, such as σ and σ_{Kubo} , only requires knowledge of the dispersion $E(P, n)$, which is a purely thermodynamic quantity! The latter may be evaluated in various limiting cases. The previously considered mJJ model can be obtained by considering a particle moving in a weakly interacting bosonic gas by taking the limit of strong repulsion between the impurity and the atoms in the background. The latter can be modeled semiclassically by a Bose–Einstein condensate as we explain in the next section. In this case the depletion parameters N and Φ are obtained directly from the solution of the Gross–Pitaevskii equation (GPE). In the case of a strongly interacting background, quantum fluctuations play a dominant role and one has to use a full quantum-mechanical calculation for the dispersion $E(P, n)$. This can be done in the extreme TG limit which is equivalent to free fermions as we show in section 6.

5. Impurity in a weakly interacting background

For the case of a weakly interacting background the energy and momentum of the impurity can be determined using the classical solution $X(t) = Vt$ of the impurity's coordinate. Here the condensate wavefunction acquires the traveling wave form $\Psi(x, t) = \Psi(x - Vt)$ in the frame moving with the impurity and satisfies the GPE

$$-iV\partial_x \Psi = -\frac{1}{2m} \partial_x^2 \Psi - g(n - |\Psi|^2)\Psi + G\delta(x)\Psi, \quad (31)$$

where g is the interaction coupling constant between the background atoms and G is the impurity-background interaction constant. Due to the presence of the repulsive contact interaction term, the moving impurity creates a depletion cloud which is effectively bound to it.



The shape of the depletion cloud can be obtained by constructing a solution from two impurity free solutions (i.e. those with $G = 0$) that satisfy the proper boundary conditions at location of the impurity: $\Psi'(0^+) - \Psi'(0^-) = 2mG\Psi(0)$. This strategy is facilitated by the fact that for $V < c$ the bare GPE ($G = 0$ in equation (31)) admits a one-parameter family of soliton [53, 54] solutions:

$$\Psi_s(x) = \sqrt{n} \left(\frac{V}{c} - i \sqrt{1 - \frac{V^2}{c^2}} \tanh \frac{x}{l} \right), \quad (32)$$

where $l^{-1} = m\sqrt{c^2 - V^2}$. The solitons can be visualized as a density dip having a core size l , as well as a corresponding phase drop. By appropriately matching two solitonic solutions at the impurity location one solves equation (31) [25] as illustrated in figure 5.

From the solution $\Psi(x - Vt)$ the equilibrium values of the collective coordinates N , Φ can be computed directly in terms of the coupling G and velocity V , as shown in figure 5. As expected, these values are in complete agreement with the thermodynamic definitions in equations (26). This can be shown by first solving for the energy $E(V, n)$ and momentum $P(V, n)$ as functions of V using the equations

$$E = MV^2/2 + \int dx \left[\frac{1}{2m} |\partial_x \Psi|^2 + \frac{g}{2} (n - |\Psi|^2)^2 \right] + G|\Psi(0)|^2, \quad (33)$$

$$P = MV + i \int dx \Psi^* \partial_x \Psi + n\Phi. \quad (34)$$

By inverting equation (34) one finds $V(P, n)$, which can be substituted into the energy to yield the dispersion $E(V(P, n), n) = E(P, n)$. The same procedure independently yields the equilibrium values of the collective coordinates $N(P, n)$, $\Phi(P, n)$ as functions of the total momentum, which allows one to check that the thermodynamic relations (26) are indeed fulfilled.

With the impurity dispersion now in hand, one can proceed to compute the nonlinear mobility σ using equation (28) and the backscattering amplitude Γ given by (30). For a weak impurity, $G \ll c$, the main contribution to equation (28) comes from the regions of momentum where the velocity is maximal $V \approx V_c \approx c$, leading to

$$\sigma \approx \frac{1}{nmG}, \quad G/c \ll 1. \quad (35)$$

which is enhanced compared to equation (13) obtained for mJJ model. This enhancement of mobility can be attributed to the fact that in the present case the impurity is almost transparent to phononic excitations.

For calculation of the backscattering amplitude we can concentrate on $P \sim 0$ region and use the perturbation theory in G/c to obtain $N \approx G/g$, $\Phi \approx PG/Mc^2$. Then equation (30) leads to the backscattering amplitude

$$\Gamma(P, n) = \frac{1}{mc^2} \left(\frac{G}{c} \right) \left(\frac{mG}{Mg} - 1 \right), \quad (36)$$

vanishing identically for the integrable case $M = m$, $G = g$.

In the case of a strongly repulsive impurity, $G \gg c$, the critical velocity $V_c = c^2/G \ll c$ is small and we have $N = 2n/mc$, $\Phi = P/n$ for essentially any momentum P , due to the small bandwidth of the impurity dispersion. The nonlinear mobility

$$\sigma \approx \frac{K}{2\pi n^2} \left(1 - \frac{1}{8} \frac{c^2}{G^2} \right), \quad G/c \gg 1. \quad (37)$$

is only slightly different from the mJJ result equation (13). For the same reason the backscattering amplitude is approximately momentum independent and given by

$$\Gamma(P, n) = \frac{1}{mc^2} \left(1 - \frac{Mc}{n} \right). \quad (38)$$

Assuming $Mc/n \ll 1$ leads to $\Gamma = 1/mc^2$ which coincides with the value $\Gamma = -K\mathcal{M}/\pi n^2$ derived in section 3.2 for the mJJ model with $\mathcal{M} = -mN = -2n/c$.

6. Impurity in a Tonks–Girardeau gas

In the case of a weakly interacting bosonic gas, the formation of the depleton and its corresponding periodic dispersion law can be understood as a consequence of the binding of a soliton to the impurity. The large number of depleted particles $N \propto K \gg 1$ allows one to develop a semiclassical description of this binding, in which the density and phase fields can be described using the mean-field GPE.

As the bosonic gas becomes more strongly interacting the number of missing particles in the depletion cloud diminishes and the mean-field description becomes inappropriate: both the soliton and its binding to the impurity must be treated quantum mechanically. As long as the impurity mass is sub-critical (see section 2) the transition from weak to strong coupling is a smooth crossover and the impurity-soliton bound state remains intact. In this section we illustrate this continuity by considering the extreme case of bosons with infinite repulsion, widely known as the TG gas [55].

One may represent the TG gas of nL hard-core bosons by free fermions with momentum creation/annihilation operators satisfying $\{c_p, c_p^\dagger\} = \delta_{pp'}$. This leads to the following Hamiltonian

$$\hat{H} = -\frac{1}{2M} \frac{\partial^2}{\partial X^2} + \sum_p \frac{p^2}{2m} c_p^\dagger c_p + \frac{G}{L} \sum_{p,q} c_p^\dagger c_{p+q} e^{iqX}. \quad (39)$$

We note that the above mapping to free fermions is valid for interactions of the density–density type, which we have assumed to be local in space.

To understand the low-energy properties of equation (39), consider a state of the system with total momentum $P > 0$. If $P < P_0 \equiv \min\{Mv_F, k_F\}$, where $k_F = \pi n$ and $v_F = k_F/m$ the low energy states are those where most of the momentum is carried by the impurity. Indeed, the impurity kinetic energy $P^2/2M$ is less than that of soft particle–hole excitations above the Fermi sea $\sim v_F P$. On the other hand, for $P > P_0$ the low energy states are those where *hole excitations* carry a significant fraction of the entire momentum P . The many-body ground state adiabatically connects between these two limits, thus signaling strong impurity-hole hybridization at $P \gtrsim P_0$. As we show below, the strong hybridization manifests itself in the formation of an impurity-hole bound state. This non-perturbative process is responsible for the smoothness of the impurity dispersion relation, which in turn gives rise to Bloch oscillations under the application of an external force.

To illustrate this effect, it is sufficient to consider a subspace of the full many-body space containing a single hole excitation with momentum $0 < k < 2k_F$, in addition to the impurity with momentum $P - k$. This restriction is justified in the limit of weak coupling, $G \ll v_F$, where the number of particle–hole pairs created by the impurity in the ground-state is suppressed. The basis vectors of this subspace are

$$|k; P\rangle = e^{i(P-k)X} c_{k_F}^\dagger c_{k_F-k} |\Psi_{\text{FS}}\rangle, \quad (40)$$

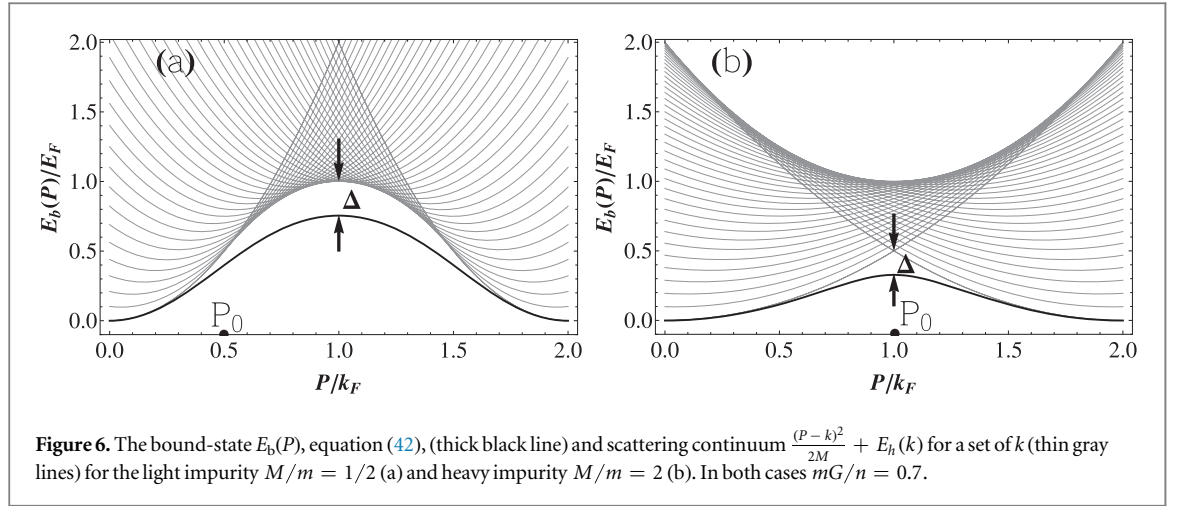
where $|\Psi_{\text{FS}}\rangle$ denotes the unperturbed Fermi sea ground-state. The corresponding Schrödinger equation $\sum_{k'} \langle k; P | \hat{H} | k'; P \rangle \psi_P(k') = E \psi_P(k)$ takes the form of a two-particle problem with an *attractive* delta-interaction (formally the attraction arises from anti-commuting the fermionic operators in the last term in equation (39)),

$$\left[\frac{(P-k)^2}{2M} + E_h(k) + nG \right] \psi_P(k) - G \int_0^{2k_F} \frac{dk'}{2\pi} \psi_P(k') = E \psi_P(k). \quad (41)$$

Here $E_h(k) = v_F k - k^2/2m$ is the hole kinetic energy (we measure E relative to $NE_F/3$). This problem admits a unique bound-state solution, whose energy $E = E_b(P) + nG$ is found from the integral equation

$$\int_0^{2k_F} \frac{dk'}{\frac{(P-k')^2}{2M} + E_h(k') - E_b(P)} = \frac{2\pi}{G}. \quad (42)$$

The resulting bound-state dispersion, shown in figure 6, is a smooth periodic function of the total momentum, which is split from the scattering continuum $E_h(k) + (P-k)^2/2M$ by the gap Δ .



The hard gap between the bound-state and the continuum is an artifact of restricting the particle in equation (40) to be created right at the Fermi momentum k_F . Allowing for slight deviations $c_{k_F}^\dagger \rightarrow c_{k_F+p}^\dagger$, enlarges the Hilbert space to include, in addition to the bound-state, low energy, $\sim v_F p$, particle-hole excitations. It is well known [36, 47, 51] that interactions with these excitations transforms the bound-state into the *quasi* bound-state with the power-law (instead of the pole) spectral function $A(P, \omega)$. These low energy excitations are also responsible for radiation losses and thus for the finite mobility σ . As long as the external force is sufficiently small, $F < F_{\max}$, they do not destroy the Bloch oscillations associated with the impurity following the quasi bound-state.

6.1. Results for the exactly integrable model $M = m$

It is worth noticing that the one-hole bound-state solution (42) is in *quantitative* agreement with the available exact results. For example, for $M = m$, the integrability of the model given by equation (39) allows one to determine the exact ground-state energy $E(P, n)$ [36]. It is defined implicitly through the integral relations

$$\begin{aligned} E(\Lambda) &= \frac{k_F^2}{2m} + \int_{-k_F}^{k_F} \frac{dk}{2\pi} \frac{4mG}{(mG)^2 + 4(k - \Lambda)^2} \left[\frac{k^2}{2m} - \frac{k_F^2}{2m} \right], \\ P(\Lambda) &= -2 \int_{-k_F}^{k_F} \frac{dk}{2\pi} \arctan \frac{2(k - \Lambda)}{mG}, \end{aligned} \quad (43)$$

where one must eliminate Λ in the upper equation using $\Lambda(P)$ from the lower equation.

In the vicinity of $P \sim k_F$, where the one-hole bound-state is expected to be valid, one finds

$$E(P \rightarrow k_F) = E_F - \frac{2\pi v_F}{3G} \frac{(P - k_F)^2}{2m}.$$

One may indeed verify from equation (42) that $E_b(P \rightarrow k_F) + nG \approx E(P \rightarrow k_F)$. The effective mass of the bound-state, $M^* = -\frac{3mG}{2\pi v_F}$, therefore agrees with the exact result (up to perturbative corrections of $\mathcal{O}(G^2)$ which are subleading for $G \ll v_F$). This shows that the single hole binding to the impurity is indeed the leading physical effect in the weak coupling limit.

At strong coupling the impurity becomes dressed by multiple particle-hole pairs and the above one-hole ansatz loses its quantitative applicability. Nevertheless, the concept of the depleton as the impurity-hole bound state is expected to survive, in the sense that the impurity drags with it a depletion cloud with precisely one missing particle (i.e., a localized hole). This statement can be made precise by studying the ground-state pair correlation function $\langle n(x) n_i(0) \rangle$, which measures the fermion density a distance x away from the impurity (here n_i is the impurity density operator).

For the integrable case $M = m$ the pair correlation function was studied analytically by McGuire [56], with the strong coupling $G \gg v_F$ result

$$\langle n(x) n_i(0) \rangle = n \left(1 - \frac{\sin^2 k_F x}{k_F^2 x^2} \right). \quad (44)$$

Integrating the deviation of equation (44) from the background density n over all space yields the number of depleted particles $N = \int_x (n - \langle n(x) n_i(0) \rangle) = 1$.

McGuire also studied the pair correlation function and ground-state energy E for arbitrary coupling, in the case of zero momentum $P = 0$. It is interesting to note that from McGuire's solution the number of depleted particles, as defined through the pair correlation function $\int_x (n - \langle n(x) n_i(0) \rangle)$, is identical to the

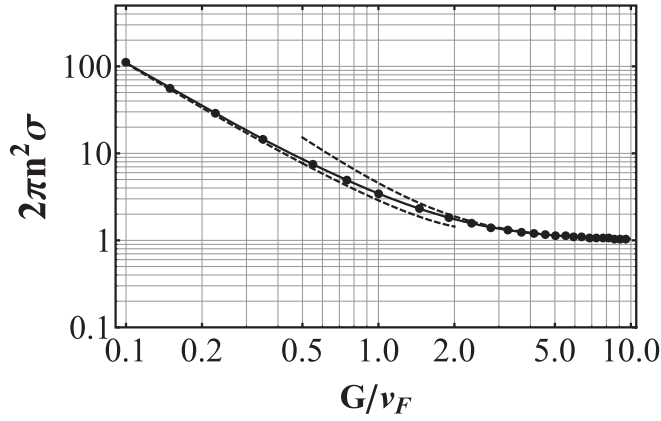


Figure 7. Nonlinear mobility for the equal mass impurity in a Tonks–Girardeau gas. The dashed lines are the asymptotic limits given by equation (46).

thermodynamic expression $\partial_\mu E$ ($\mu = \frac{k_F^2}{2m}$ is the chemical potential of the background fermions)

$$N = \partial_\mu E = \int_x (n - \langle n(x)n_i(0) \rangle) = \frac{2}{\pi} \arctan \frac{G}{2v_F}. \quad (45)$$

This result substantiates our intuition that N , as defined through the thermodynamic relation (26) (at $P = 0$ in the present case), is indeed related to the real space depletion of particles in the vicinity of the impurity, despite the absence of its semiclassical description. The corresponding lengthscale ξ of the depletion cloud is of course just the Fermi wavelength, see equation (44), in agreement with the general expectation $\xi = 1/mc$ [25] where $c = v_F$.

6.2. Exact nonlinear mobility

The above results confirm the idea that the ground-state properties of the model can be understood in terms of the impurity-hole bound state. The dynamic response of the bound-state can be described within the depletion framework of section 4, where it was discussed that the response to an external force F , can be characterized by the purely thermodynamic quantity $E(P, n)$. By computing the dispersion from the integral equation (43) we may determine the exact mobility using equations (26) and (28). At weak or strong coupling the mobility is given by

$$\sigma = \frac{1}{2\pi n^2} \begin{cases} \frac{4v_F^2}{G^2 \ln \frac{4v_F}{G}}, & G \ll v_F; \\ 1 + \frac{32}{9} \frac{v_F^2}{G^2}, & G \gg v_F. \end{cases} \quad (46)$$

These asymptotic formulae provide rather tight bounds on the exact mobility deduced numerically from the integral equations (43), as shown in figure 7. One can arrive to equation (46) in the limit of strong coupling $G \gg v_F$ by expanding the functions $V(P, n)$, $N(P, n)$, $\Phi(P, n)$ to the leading order in v_F/G . Substitution of the resulting expressions into equation (28) gives the second line of equation (46).

In the limit of weak coupling the dispersion acquires a more complicated form: it consists of essentially unperturbed parabolae centered at momenta $P = 2jk_F$ for integer j with weak anti-crossings at $P = (2j + 1)k_F$. The value of the collective coordinates $N(P, n)$, $\Phi(P, n)$ thus remain close to zero at small momentum $P < k_F$ and change rapidly to $(N, \Phi/\pi) \rightarrow 1$ in the vicinity of k_F in a window of width mG . The momentum derivatives $(\partial_P N, \partial_P \Phi/\pi)$ which enter the mobility formula (28) are strongly peaked at $P = k_F - mG/2$, with height $\propto 1/mG$. One may thus approximate for $G \ll v_F$

$$\begin{aligned} \sigma &\approx \int_{k_F - mG/2}^{k_F} \frac{dP}{n} \frac{(\partial_P N)^2}{1 - V^2/v_F^2} \sim \frac{1}{nmG} \frac{1}{1 - V^2(k_F - mG/2)/v_F^2} \\ &\sim \frac{1}{n^2} \frac{v_F^2}{G^2 \ln(4v_F/G)}, \end{aligned} \quad (47)$$

where $V(k_F - mG/2)/v_F \approx 1 - \frac{G}{2\pi^2 v_F} \ln \frac{4v_F}{G}$ can be obtained from second order perturbation theory, see e.g. equation (2) of [36], and essentially coincides with $V_c \approx v_F$ in this limit (at strong coupling $V_c = 2v_F^2/3G$).

Keeping track of the numerical prefactor in equation (47) leads to the first line of equation (46). Deviations away from the integrable point $M = m$ do not significantly affect equation (46) provided $|1 - M/m| < G/v_F$. As we shall see in the next section, however, the backscattering amplitude, and thus the Kubo mobility, is strongly sensitive to the deviation from integrability.

6.3. Backscattering amplitude

As shown previously [23, 25] the backscattering amplitude vanishes at points of exact integrability. For the TG gas this implies that $\Gamma \propto 1 - M/m$ when $M \sim m$. Below we verify this behavior and obtain the exact prefactor in various limiting cases where the analytic form is available.

In the limit of strong coupling we may set $N = 1$ and neglect terms proportional to $1/M^* \propto 1/G$ in equation (30). We then find

$$\Gamma = -\frac{\pi}{mv_F^2} \left(\frac{M}{m} - 1 \right), \quad G \gg v_F. \quad (48)$$

This result is independent of momentum to leading order, owing to the essentially flat dispersion with bandwidth $\propto 1/G$.

At small coupling the backscattering amplitude acquires a complicated momentum dependence and we restrict ourselves to its behavior in the vicinity of the analytically accessible points $P = 0, k_F$. At small momentum one may resort to second order perturbation theory to obtain $E(P, n) \approx P^2/2M^* + \mu_d$ with $M^*(P = 0) = M(1 + (G/\pi v_F)^2)$ and $\mu_d = nG$. Substituting this dispersion into equation (30) gives

$$\Gamma(P = 0) = -\frac{2\pi}{mv_F^2} \left(\frac{G}{\pi v_F} \right)^2 \left(\frac{M}{m} - 1 \right), \quad G \ll v_F. \quad (49)$$

At $P = k_F$ we instead use $E(P = k_F) \approx \frac{k_F^2}{2M}$ and neglect terms of order $(M - mN)/M^*(P = k_F) \ll 1$. Recalling that $M^*(P = k_F) \propto -mG/v_F$, these approximations are seen to be valid for small deviations away from the integrable point, $|1 - M/m| < G/v_F \ll 1$. Substituting them into equation (30) gives

$$\Gamma(P = k_F) = -\frac{2\pi}{mv_F^2} \left(\frac{M}{m} - 1 \right), \quad G \ll v_F. \quad (50)$$

In all cases the backscattering amplitude scales as $1 - M/m$, thus vanishing at the exactly integrable point $M = m$. This implies the vanishing of the thermal viscosity and the divergence of the Kubo mobility σ_{Kubo} at finite temperature. In this case the response to even an infinitesimal external force is nonlinear: the velocity exhibits Bloch oscillations superimposed with the drift $V_D = \sigma F$.

7. Impurity in a trapped condensate

We now consider the dynamics of an impurity coupled to a 1D quantum liquid confined by a weak harmonic potential $V(x) = \frac{1}{2}m\omega^2 x^2$ with $\omega \ll \mu$, where μ is the chemical potential of the 1D gas in the trap center. In this case the spatial extent L of the gas is much larger than the healing length ξ and one may use the local density approximation (LDA), for which the local chemical potential is given by $\mu(x) = \mu - \frac{1}{2}m\omega^2 x^2$ for

$|x| < \sqrt{\frac{2\mu}{m\omega^2}} \equiv L$, while $\mu(x) = n(x) = 0$ for $|x| > L$. In the LDA, one first solves the homogeneous problem at fixed density for the depleton dispersion law $E(P, n)$ and then substitutes in it the local density $n(X)$ to obtain the adiabatic depleton Hamiltonian

$$H_{\text{trap}}(P, X) = E(P, n(X)) + \frac{1}{2}M\omega_I^2 X^2. \quad (51)$$

Here we introduced an additional harmonic potential, acting on the impurity only, as a control field that can tune the system into different regimes of stability (this can be achieved using e.g. a species or state selective potential).

In the limit $\omega_I \rightarrow \infty$ the impurity is strongly localized in the trap center, while for $\omega_I \rightarrow 0$ it is instead expelled from the center by the repulsive potential produced by the inhomogeneous density profile of the host particles. The transition between these two regimes occurs at a critical value of the trapping frequency, which can be deduced by expanding equation (51) in small deviations away from $X = P = 0$

$$H_{\text{trap}}(P, X) \approx \frac{P^2}{2M^*} + \frac{1}{2}(M\omega_I^2 - mN\omega^2)X^2 + E_0, \quad (52)$$

where we used equation (26) and defined $E_0 = E(0, N)$ (note that the inverse effective mass $1/M^* = \partial_P^2 E$ is distinct from $1/M$ used above, see e.g. equation (4)). From equation (52) we see that both the impurity mass and trapping potential are renormalized by interactions with the background particles, and act to make the motion

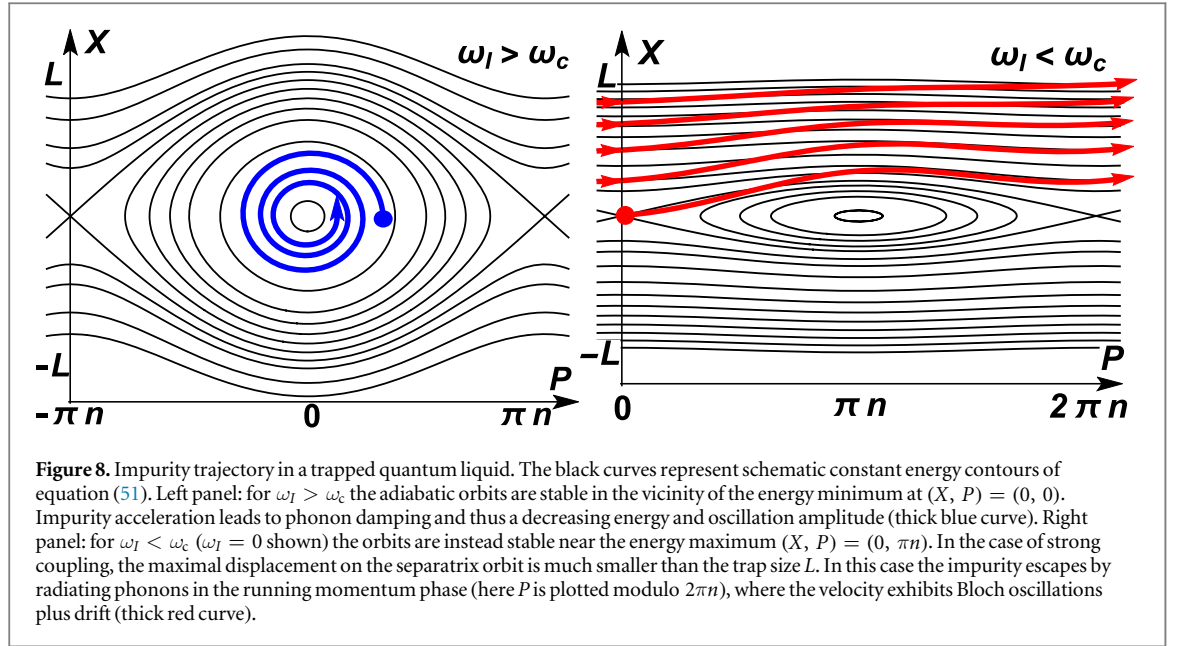


Figure 8. Impurity trajectory in a trapped quantum liquid. The black curves represent schematic constant energy contours of equation (51). Left panel: for $\omega_I > \omega_c$ the adiabatic orbits are stable in the vicinity of the energy minimum at $(X, P) = (0, 0)$. Impurity acceleration leads to phonon damping and thus a decreasing energy and oscillation amplitude (thick blue curve). Right panel: for $\omega_I < \omega_c$ ($\omega_I = 0$ shown) the orbits are instead stable near the energy maximum $(X, P) = (0, \pi n)$. In the case of strong coupling, the maximal displacement on the separatrix orbit is much smaller than the trap size L . In this case the impurity escapes by radiating phonons in the running momentum phase (here P is plotted modulo $2\pi n$), where the velocity exhibits Bloch oscillations plus drift (thick red curve).

of the impurity slower (generally $N > 0$ and $M^* > M$ near $P = 0$). The effective oscillation frequency of the impurity is

$$\Omega = \sqrt{\frac{M\omega_I^2 - mN\omega^2}{M^*}} < \omega_I. \quad (53)$$

As one lowers ω_I , the oscillation frequency Ω decreases and crosses zero at the critical value of the trapping frequency

$$\omega_c = \sqrt{\frac{mN}{M}} \omega. \quad (54)$$

This signals the frequency at which the trap center near $P = 0$ becomes an unstable maximum and here Ω becomes purely imaginary (illustrated by the saddle point in figure 8 for $\omega_I < \omega_c$). Setting $\omega_I = 0$ for simplicity, we see that in the limit of weak coupling, $G \ll c$, the lifetime of the impurity initiated at rest in the trap center can be estimated as $\text{Im } \Omega^{-1}$ using equation (53). This is appropriate because the maximal displacement from the center on the separatrix orbit is already roughly the trap size: $X \sim \sqrt{\frac{E_\pi - E_0}{mN\omega^2}} \sim L$, ($E_\pi - E_0 \sim \mu N$ at weak coupling), thus allowing the impurity to reach the trap edge and escape.

At strong coupling, however, the maximal displacement on the separatrix is much smaller, $X \sim L\sqrt{c/G} \ll L$, owing to the small impurity bandwidth, $E_\pi - E_0 \sim \mu N (c/G)$, see figure 8. This implies that the impurity becomes ‘self-trapped’ in a high energy metastable state by the background gas, and can only escape by releasing energy into phonon excitations. This dissipation allows the impurity to rapidly cross the separatrix and enter the running momentum phase, accompanied by a drift towards the trap edge and small amplitude Bloch oscillations in the velocity, shown by the thick red curve in figure 8. Here, Bloch oscillations are driven by the gradient of the inhomogeneous density profile of the gas. The timescale and trajectory of the escape can be estimated by noting that since the force is an increasing function of the displacement, $F = -\partial_X H_{\text{trap}} \sim mN\omega^2 X$, the displacement, in turn, satisfies the differential equation $\dot{X} = \sigma F \sim \frac{\omega^2}{\mu} X$ (at strong coupling $\sigma = \frac{1}{2nm\epsilon}$, and one can neglect the amplitude of velocity oscillations). This leads to the exponential increase of the impurity displacement, $X(t) \propto e^{\omega^2 t/\mu}$, on the timescale $\mu/\omega^2 \sim 170$ ms for the parameters used in the experiment of [18], discussed below. We note that in the extreme limit $G \rightarrow \infty$ ($V_c \rightarrow 0$) the impurity cannot escape, since the number of particles in the left and right condensates become conserved quantities. This implies that the lifetime of the trapped impurity sharply increases beyond μ/ω^2 as a function of coupling, once $mV_c < 1/L$. For the system studied in [18] this yields a crossover coupling ($G/g \sim 100$) that greatly exceeds the experimental values, so we do not pursue this special limit further.

The above results can be tested experimentally by localizing an impurity in the center of a trapped gas, and measuring the width of the subsequent impurity distribution $\langle X^2(t) \rangle$ as a function of time. This was done in [18] using a species selective dipole potential to initialize a ^{41}K impurity in a gas of moderately interacting ^{87}Rb atoms ($mg \sim n$). The ratio of the trapping frequencies was fixed at $\omega_I/\omega = 1.3$, while the K–Rb scattering length was

varied by a magnetic field using a Feshbach resonance. From equation (54) we find a critical coupling strength given by $N_c \sim G_c/g = M\omega_I^2/m\omega^2 \sim 1$, above which we have $\omega_I < \omega_c$ and below $\omega_I > \omega_c$.

At stronger coupling, $G > g$, we thus expect the self-trapping behavior to become pronounced, which appears consistent with the results of [18] showing a rapid decrease of the initial oscillation amplitude for $G > g$ (see figure 4 of [18]). The characteristic timescale for the increase of the width at the largest coupling in [18] ($G/g = 30$) is a factor of ~ 8 faster than μ/ω^2 . Aside from a possible numerical prefactor (that goes beyond the accuracy of the above discussion), this discrepancy could also be explained by the fact that the temperature in [18] is rather large $T \sim \mu$, making the thermal dissipation channel highly relevant (the system is far from integrability due to the K–Rb mass difference), thus giving a faster decay time. The high temperature makes a quantitative comparison with [18] difficult since at weak coupling $G \ll g$, T is already substantially larger than the K–Rb interaction energy $nG \ll T$, while at strong coupling $G/c \gg 1$ the temperature is comparable to or exceeds the impurity bandwidth $T > nV_c$. Accessing lower temperatures, or perhaps closeness to integrability (using e.g. internal hyperfine states of Rb) would make a direct quantitative comparison to the above theoretical results possible (see also [57–59] for different approaches to the problem of a quantum impurity in a trapped gas).

8. Conclusions and open questions

In this paper we have provided an overview of the physics of mobile impurities in 1D quantum liquids using the simplified mobile JJ model and generalizing it to the phenomenological *depleton* model. Our description is based on the existence of the equilibrium dispersion relation $E(P, n)$, defined as the ground state of the combined system of an impurity and the superfluid background, at a given momentum P and background density n . This dispersion curve can be understood in terms of the thermodynamics of a quantum liquid flowing past an impurity. We have exploited the periodicity properties of the dispersion to predict the existence of adiabatic Bloch oscillations in the absence of an underlying lattice. The interaction of the mobile impurity with low energy phononic excitations was described in terms of two slow collective variables, which allowed us to address, in particular, the effects of dissipation and dephasing. Based on these results, we were able to show that the dynamics of impurities in uniform and trapped systems can be fully characterized.

Using our exact general results, we have provided model-specific calculations of the linear (Kubo) and nonlinear mobilities in the tractable limits of a weakly interacting and a strongly interacting background. It is interesting to see that both these limits lead to a clear physical picture of a depleton consisting of the repulsive impurity binding to an effective ‘hole’ in the background. In this way the depleton properties, such as the effective mass, become strongly interaction and momentum dependent.

A spinless particle interacting with a scalar background represents the simplest case of a mobile impurity. Including internal degrees of freedom of the impurity and those of the background particles are expected to change *qualitatively* the low energy physics, like in the case of spin 1/2 impurity moving in the background made of spin 1/2 fermions [60]. In this case the spin-spin interactions become singular at low energy due to the formation of a Kondo polaron and lead to the mobility behaving as T^{-2} at low temperatures. Extending these studies to bosonic backgrounds and other values of spin may result in interesting effects of entanglement and strong correlations which can be probed experimentally by radio-frequency pulses.

Our description was limited to small applied forces and low temperatures, where the concept of remaining close to the equilibrium zero-temperature dispersion remains meaningful. One open question is to understand to what extent our results apply to the cases of stronger forces or higher temperatures that are typical of current experiments in ultracold atoms. Another open question is the physics of depleton formation relevant at initial stages of dynamical experiments with impurities.

Acknowledgments

The authors would like to thank A Lamacraft, M Zvonarev, M Knap, E Demler, O Lychkovskiy, O Gamayun, V Cheianov, T Giamarchi, I V Lerner and B Horovits for many enlightening conversations that have contributed to our understanding of impurity dynamics in reduced dimensions. A K was supported by NSF grant DMR1306734. MS was supported by the Danish National Research Foundation and The Danish Council for Independent Research—Natural Sciences. M S and D M G gratefully acknowledge the hospitality of the University of Minnesota.

References

- [1] Daunt J G, Probst R E, Johnston H L, Aldrich L T and Nier A O 1947 *Phys. Rev.* **72** 502

- [2] Landau L D and Pomeranchuk I 1948 *Dokl. Akad. Nauk* **59** 669
- [3] Landau L D and Khalatnikov I M 1949a *Zh. Eksp. Teor. Fiz.* **19** 637
- [4] Landau L D and Khalatnikov I M 1949b *Zh. Eksp. Teor. Fiz.* **19** 709
- [5] Khalatnikov I M and Zharkov V N 1957 *Sov. Phys.—JETP* **5** 905
- [6] Bardeen J, Baym G and Pines D 1966 *Phys. Rev. Lett.* **17** 372
- [7] Baym G 1966 *Phys. Rev. Lett.* **17** 952
- [8] Baym G 1967 *Phys. Rev. Lett.* **18** 71
- [9] Bardeen J, Baym G and Pines D 1967 *Phys. Rev.* **156** 207
- [10] Baym G and Ebner C 1967 *Phys. Rev.* **164** 235
- [11] Abraham B M, Eckstein Y, Ketterson J B and Vignos J H 1966 *Phys. Rev. Lett.* **17** 1254
- [12] Golub R and Pendlebury J M 1975 *Phys. Lett. A* **53** 133
- [13] Golub R and Penlebury J M 1977 *Phys. Lett. A* **62** 337
- [14] Golub R 1979 *Phys. Lett. A* **72** 387
- [15] Palzer S, Zipkes C, Sias C and Köhl M 2009 *Phys. Rev. Lett.* **103** 150601
- [16] Pilch K, Lange A D, Prantner A, Kerner G, Ferlaino F, Nägerl H-C and Grimm R 2009 *Phys. Rev. A* **79** 042718
- [17] Spethmann N, Kindermann F, John S, Weber C, Meschede D and Wiedera A 2012 *Appl. Phys. B* **106** 513
- [18] Catani J, Lamporesi G, Naik D, Gring M, Inguscio M, Minardi F, Kantian A and Giamarchi T 2012 *Phys. Rev. A* **85** 023623
- [19] Zipkes C, Palzer S, Sias C and Köhl M 2010 *Nature* **464** 388
- [20] Zipkes C, Palzer S, Ratschbacher L, Sias C and Köhl M 2010 *Phys. Rev. Lett.* **105** 133201
- [21] Schmid S, Härter A and Denschlag J H 2010 *Phys. Rev. Lett.* **105** 133202
- [22] Fukuhara T *et al* 2013 *Nat. Phys.* **9** 235
- [23] Gangardt D M and Kamenev A 2009 *Phys. Rev. Lett.* **102** 70402
- [24] Gangardt D M and Kamenev A 2010 *Phys. Rev. Lett.* **104** 190402
- [25] Schecter M, Gangardt D M and Kamenev A 2012 *Ann. Phys.* **327** 639
- [26] Schecter M, Kamenev A, Gangardt D M and Lamacraft A 2012 *Phys. Rev. Lett.* **108** 207001
- [27] Mathy C J M, Zvonarev M B and Demler E 2012 *Nat. Phys.* **8** 881
- [28] Knap M, Mathy C J M, Ganahl M, Zvonarev M B and Demler E 2014 *Phys. Rev. Lett.* **112** 1
- [29] Burovski E, Cheianov V, Gamayun O and Lychkovskiy O 2014 *Phys. Rev. A* **89** 041601
- [30] Gamayun O, Lychkovskiy O and Cheianov V 2014 *Phys. Rev. E* **90** 032132
- [31] Lychkovskiy O 2015 *Phys. Rev. A* **91** 040101
- [32] Schecter M, Gangardt D M and Kamenev A 2015 *Phys. Rev. E* **92** 016101
- [33] Gamayun O, Lychkovskiy O and Cheianov V 2015 *Phys. Rev. E* **92** 016102
- [34] Castelnovo C, Caux J-S and Simon S H 2016 *Phys. Rev. A* **93** 013613
- [35] Devoret M H, Wallraff A and Martinis J M 2004 arXiv:cond-mat/0411174
- [36] Lamacraft A 2008a *Phys. Rev. B* **79** 241105
- [37] Caldeira A O and Leggett A J 1983 *Ann. Phys.* **149** 374
- [38] Astrakharchik G E and Pitaevskii L P 2004 *Phys. Rev. A* **70** 13608
- [39] Büchler H P, Geshkenbein V B and Blatter G 2001 *Phys. Rev. Lett.* **87** 100403
- [40] Kane C L and Fisher M P A 1992 *Phys. Rev. B* **46** 15233
- [41] Castro Neto A H and Fisher M P A 1996 *Phys. Rev. B* **53** 9713
- [42] Giamarchi T 2004 *Quantum Physics in One Dimension* (Oxford: Oxford University Press)
- [43] Kamenev A 2011 *Field Theory of Non-Equilibrium Systems* (Cambridge: Cambridge University Press)
- [44] Gamayun O 2014 *Phys. Rev. A* **89** 063627
- [45] Khodas M, Pustilnik M, Kamenev A and Glazman L I 2007 *Phys. Rev. Lett.* **99** 110405
- [46] Khodas M, Kamenev A and Glazman L I 2008 *Phys. Rev. A* **78** 53630
- [47] Kamenev A and Glazman L I 2009 *Phys. Rev. A* **80** 11603
- [48] Imambekov A and Glazman L I 2008 *Phys. Rev. Lett.* **100** 206805
- [49] Imambekov A and Glazman L I 2009 *Science* **323** 228
- [50] Zvonarev M B, Cheianov V V and Giamarchi T 2009 *Phys. Rev. B* **80** 201102
- [51] Imambekov A, Schmidt T and Glazman L 2012 *Rev. Mod. Phys.* **84** 1253
- [52] Campbell A S 2013 Mobile impurities in one-dimensional quantum liquids *PhD Thesis* University of Birmingham
- [53] Pitaevskii L P and Stringari S 2003 *Bose–Einstein Condensation* (Oxford: Clarendon)
- [54] Tsuzuki T 1971 *J. Low Temp. Phys.* **4** 441
- [55] Girardeau M 1960 *J. Math. Phys.* **1** 516
- [56] McGuire J B 1965 *J. Math. Phys.* **6** 432
- [57] Bonart J and Cugliandolo L F 2013 *Europhys. Lett.* **101** 16003
- [58] Peotta S, Rossini D, Polini M, Minardi F and Fazio R 2013 *Phys. Rev. Lett.* **110** 015302
- [59] Volosniev A G, Fedorov D V, Jensen A S, Valiente M and Zinner N T 2014 *Nat. Commun.* **5** 5300
- [60] Lamacraft A 2008b *Phys. Rev. Lett.* **101** 225301
- [61] Maslov D L and Stone M 1995 *Phys. Rev. B* **52** R5539